Impacts of Local Dimming Algorithms on the Halo Effect in LCD With Local Dimming Mini-LED Backlight

Shuai-Shuai Zhou, Han Gao, Yu-Jiao Ruan, Jian-Bang Zhuang, Yi-Jun Lu, Zhong Chen, and Wei-Jie Guo, *Member, IEEE*

***Abstract*—The local dimming mini-LED backlight has become one of the most important technologies for liquid crystal display (LCD), facilitating the improvement on high dynamic range (HDR) and power saving. The halo effect still limits the performance of LCDs employing mini-LED backlight. The impact of the number of local dimming zones on the contrast ratio has been investigated. The halo effect has also been investigated under four typical local dimming algorithms and different local dimming zones. It has been experimentally demonstrated that the halo area gradually shrinks with increasing the number of local dimming zones, contributing to the improvement on the HDR of LCD.**

***Index Terms*—Mini-LED, local dimming algorithms, halo effect, contrast ratio.**

I. Introduction

HIGH dynamic range (HDR) has become one of the important performances pursued by the next-generation display technologies [1], [2], [3], [4]. In order to present the vivid details in the displayed images, HDR displays require a contrast ratio (CR) exceeding 10^5:1 [3], [4], [5]. Currently, liquid crystal display (LCD) and organic light-emitting diode (OLED) display act as the mainstream display technologies [5], [6]. Given that the traditional backlight in LCD is normally on, the light leakage through the liquid crystal panel causes the non-zero brightness of LCD at the dark state, limiting the CR seriously. OLED can achieve a genuine dark state owing to the feature of the self-emissive display. However, the lifetime of OLED display under high brightness is still limited [5], [7]. Until now, LCD still acts as the dominant display technology in high-reliability applications, such as digital signage displays, TV, and cockpit displays, among others. In order to improve the HDR and uniformity of brightness at low grayscale of LCD [8], dimmable backlight has been proposed, including global dimming [9], [10], [11] and local dimming [12], [13], [14], [15], [16], [17], [18], [19]. Global dimming controls the luminance of the backlight according to the grayscale of the displayed image. The local dimming backlights can effectively suppress light leakage in the dark state, thereby improving the HDR of LCDs effectively.

With the development of LED technology, micro-LED and mini-LED have become the important light sources for high-performance displays [20]. The size of micro-LED is less than 100 μm, and that of mini-LED is 100 to 200 μm [21], [22]. Employing mini-LEDs as the light source can enlarge the number of zones in the local dimming backlight, hence strengthening the HDR. Furthermore, taking the advantage of narrow spectra, quantum dot (QD) films have been employed in mini-LED backlight to convert the light from the array of blue mini-LEDs into tri-color mixed white light [23], [24], [25]. Uneven thickness of QD color conversion film will further improve mini-LED backlight uniformity [26]. The applications of Cd-based and InP-based QDs in mini-LED backlight have been investigated [27].

Local dimming divides the displayed image into multiple independent blocks according to the distribution of regions of mini-LEDs in the backlight, and the backlight luminance (BL) of each region will be controlled independently according to the characteristic value of the corresponding local image. The discontinuity in BL between the adjacent region may lead to a distortion of the displayed image. Therefore, various local dimming algorithms have been employed to determine the BL values and pixel compensation [1], [13], [14], [28], [29], [30]. Due to the uneven distribution of BL and light leakage from the liquid crystal panel [3], [4], [31], the halo effect seriously affects the performances of LCD employing local dimming mini-LED backlight. In the past, the researches on the halo effect of LCD with local dimming mini-LED backlight were mostly based on simulation, and the investigations based on the practical test were still lacking. Testing according to multiple methods helps to

Manuscript received 7 December 2023; revised 5 January 2024; accepted 18 January 2024. Date of publication 23 January 2024; date of current version 13 February 2024. This work was supported in part by the National Natural Science Foundation of China under Grants 62275227, 62274138, and 11904302, in part by the Science and Technology Project of Fujian Province under Grants 2023H4028 and 2023H6038, and in part by the Key Research and Industrialization Projects of Technological Innovation of Fujian Province under Grant 2022G043. *(Shuai-Shuai Zhou and Han Gao contributed equally to this work.) (Corresponding authors: Jian-Bang Zhuang; Wei-Jie Guo.)*

Shuai-Shuai Zhou, Han Gao, Yi-Jun Lu, Zhong Chen, and Wei-Jie Guo are with the National Innovation Platform for the Fusion of Industry and Education in Integrated Circuits, Department of Electronic Science, School of Electronic Science and Engineering, Xiamen University, Xiamen 361005, China (e-mail: wjguo@xmu.edu.cn).

Yu-Jiao Ruan is with the Xiamen Institute of Measurement and Testing, Xiamen 361004, China.

Jian-Bang Zhuang is with the AUO (Xiamen) Company Ltd., Xiamen 361102, China (e-mail: maxjuang@auo.com).

Digital Object Identifier 10.1109/JPHOT.2024.3357063

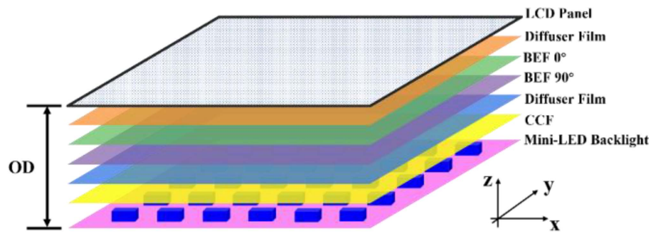

Fig. 1. Stack of mini-LED backlight LCD.

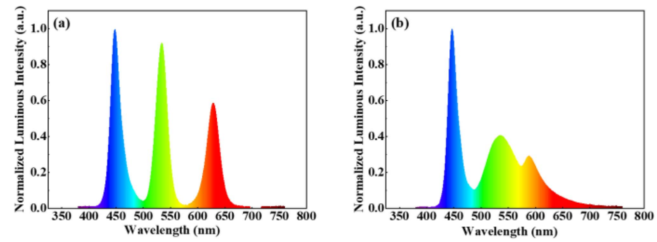

Fig. 2. Normalized spectra of (a) white image of LCD with mini-LED backlight, (b) white image of LCD with original edge-lit backlight.

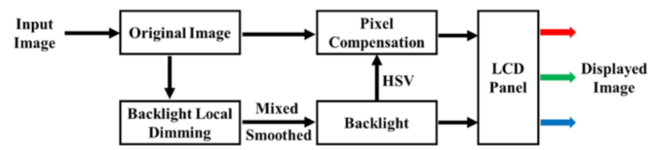

Fig. 3. Flow diagram of the local dimming LCD in this work.

speed up the desired results, promotes the integration of multiple independently controlled local dimming areas, can achieve high contrast, effectively suppress crosstalk, and further improve optical performance, which has irreplaceable advantages [32], [33], [34], [35]. In this work, and the impacts of typical BL value extraction algorithms and the number of local dimming regions on the halo effect have been investigated experimentally.

II. Design and Experiments

A. Mini-LED Backlight

The 2.8-inch local dimmable LCD has been achieved by replacing the original edge-lit backlight with the local dimming mini-LED backlight. The original LCD possesses a resolution of 240 × 320. The structure of the mini-LED backlight is shown in Fig. 1. The mini-LED backlight contains independently controlled 96 mini-LEDs, which are set into 96, 24, and 6 local dimming zones, respectively (each zone includes 1, 4, and 16 mini-LEDs). The backlight also employs a color conversion film (QF-7054FR, Guanghong Optoelectronics Co., Ltd), vertically assembled two brightness enhancement films (PS125ET-50, Jizhi Technology Co., Ltd), an upper diffuser film, and a bottom diffuser film. The package of InGaN blue mini-LEDs (MBL-B14BB75S, NationStar) contains four serially connected mini-LED chips. The driver ICs (TLC5947, Texas Instruments) have been employed to control the currents of mini-LEDs. A control board (STM32F429, STMicroelectronics) has been utilized to control the signals of LCD and backlight. Since the optical distance (OD) between the backlight and the LCD panel is required to eliminate hotspot and achieve the uniform luminance distribution [36], the OD is set at 6 mm in this work. The spectra of blue mini-LEDs and LCD have been measured by using a spectral color illuminance meter (SPIC-200, Everfine), and the normalized spectra are shown in Fig. 2. The luminance of LCD has been measured by using the spectroradiometer (CS-2000A, Konica Minolta). The luminance distributions have been collected by using imaging luminance meter (LMK6, TechnoTeam).

The flow diagram of the local dimming LCD has been illustrated in Fig. 3. BL value extraction and pixel compensation are the two primary procedures in the local dimming display. When the original image is obtained, the gray image is computed based on (1), and the low-resolution BL value would be determined according to the local dimming algorithm. Then the bilinear interpolation and low-pass filtering are utilized to accomplish the full-resolution backlight distribution with the Blur-mask Approach approach [37]. The pixel-compensated image is generated by pixel-by-pixel correction of the luminance component in Hue-Saturation-Value (HSV) space, and then the BL value is utilized to regulate the luminance of the mini-LED through pulse width modulation (PWM), generating the final image on the LCD panel.

$$Y = 0.229R + 0.587G + 0.114B. \tag{1}$$

B. BL Value Extraction Algorithm

Four mainstream local dimming algorithms, namely, maximum (MAX) method, average (AVG) method, correction (CORR) method, and inverse of mapping function (IMF) method, have been adopted and investigated.

The MAX method controls the mini-LED backlight according to the maximum gray value of the pixels in each image block. The BL value is determined according to

$$BL_{\max} = \max\left(L\left(i,j\right)\right). \tag{2}$$

where L(i,j) denotes the gray value at the pixel (i,j).

The AVG method calculates the BL values through the average gray value of the pixels of the image block. The BL value extraction is obtained by

$$BL_{avg} = \frac{1}{m \times n} \sum_{i=1}^{n} \sum_{j=1}^{m} L\left(i,j\right). \tag{3}$$

where m and n are the number of pixels corresponding to the horizontal and vertical directions of the image block, respectively.

The CORR method is a parameter-based algorithm, which enhances BL values through the difference between the maximum and average luminance of image, effectively reducing clipping artifacts and power consumption. The BL value is calculated from

$$\begin{cases} correction = \frac{1}{2}\left(Diff + \frac{Diff^2}{2^n}\right) \\ BL_{cor} = BL_{avg} + correction \end{cases} \tag{4}$$

where *Diff* denotes the difference between the maximum and average luminance, and *n* denotes the bit of gray scale.

The IMF method employs a backlight luminance modulation approach based on the histogram. The probability density function (PDF) is obtained by calculating the global histogram of the input image, and the grayscale values of the PDF are accumulated to generate a cumulative distribution function (CDF). Then, employing the line $y = x$ as the symmetry line, the CDF curve is mirrored to produce the IMF mapping function. The IMF method can customize the backlight mapping curve based on the input image, adapting to different images. In this work, after the converted gray value of the pixels in each image block has been obtained according to the IMF mapping function, BL value is calculated following

$$BL_{IMF} = 0.9 \times BL_{\max(converted)} + 0.1 \times BL_{\mathrm{avg}(converted)}. \tag{5}$$

C. Pixel Compensation

In general, the luminance of LCD perceived by human eyes is determined by the product of backlight luminance and transmissivity of LCD panel [38]. The luminance of LCD should be set to meet the ideal gamma characteristics according to [12], [38]

$$Y_{ideal}\ (g) = \left(\frac{g}{255}\right)^{\gamma}. \tag{6}$$

where g denotes the gray level and γ is a coefficient. Generally, the local dimming of the backlight will result to the reduction of the overall luminance of LCD, leading to the image distortion or the noticeable loss of detail. Therefore, the pixel compensation for the displayed images is necessary. Based on the luminance maintenance and gamma correction [39], LCD luminance compensation signal (GL_{HDR}) could be obtained through [12], [28], [40]

$$GL_{HDR} = \left(\frac{BL_{full}}{BL_{HDR}}\right)^{1/\gamma} \times GL_{Original}. \tag{7}$$

where BL_{full} and BL_{HDR} denote the intensity of traditional full-on backlight and the local dimming backlight, respectively. $GL_{Original}$ represents the original luminance of the target image. The GL_{HDR} value may exceed 255 after luminance compensation, namely the clipping effect, resulting in the loss of the image details. In order to suppress the clipping effect, the optimizations on local dimming algorithms have been proposed [41].

III. Resuts and Discussion

A. Contrast Ratio

The definition of CR is ratio of the maximum luminance to the minimum luminance of display. The HDR characteristics of LCD with local dimming backlights, which employ different numbers of local dimming zones, have been investigated according to the CR measured under the four testing patterns in Fig. 4.

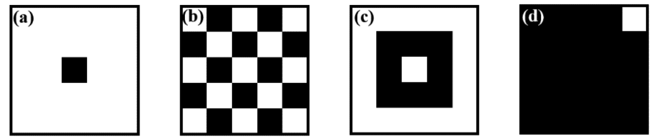

Fig. 4. Four testing patterns for CR, (a) Pattern I, (b) Pattern II, (c) Pattern III, and (d) Pattern IV.

TABLE I
Measured CR Under Four Testing Patterns Illustrated in Fig. 4

CR	Pattern			
	I	II	III	IV
6 Local Dimming	838.74	1024.49	5022.37	8852.13
24 Local Dimming	368.64	448.24	584.69	38196.04
96 Local Dimming	261.92	288.75	372.47	67526.31

TABLE II
Measured CR Under Four Testing Patterns of Original Edge-Lit LCD

CR	Pattern			
	I	II	III	IV
6 Checkerboards	420.67	502.68	664.87	688.42
24 Checkerboards	337.48	445.92	477.92	730.17
96 Checkerboards	242.38	385.38	410.92	753.01

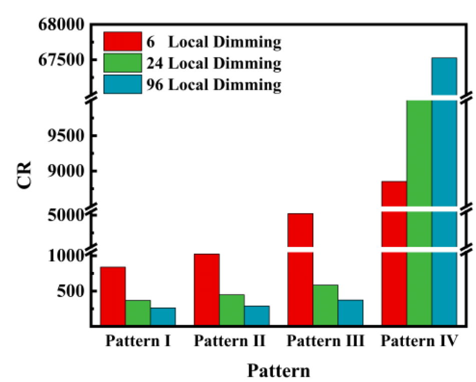

Fig. 5. CR under four testing patterns of LCD with local dimming mini-LED backlight.

As shown in Tables I, II and Fig. 5, the number of local dimming zones and the testing pattern both affect the values of CR. Since the halo effect significantly affects the luminance of the dark area surrounded or neighbored by bright area and then reduce the value of CR, the CR of patterns I-III, in which black and white squares are arranged in cross, is less than that of pattern IV. In the pattern IV, the luminance in the center of pattern is nearly unaffected by the halo effect due to that the white square is far away from the center of black region.

In patterns I-III, CR decreases as the number of local dimming zones increases. Furthermore, among patterns I-III, pattern I

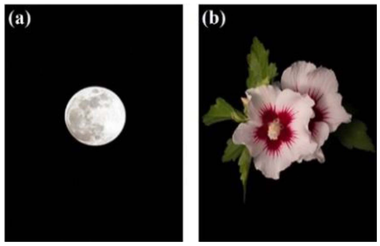

Fig. 6. Two high CR pictures (a) Moon, and (b) Flower.

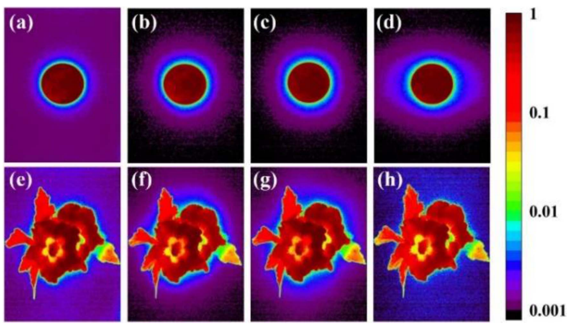

Fig. 7. Normalized luminance distributions of the two pictures displayed on the original edge-lit LCD and the LCD with mini-LED backlight under different local dimming zones. (a), (e) The original edge-lit LCD, and (b), (f), (c), (g), and (d), (h) are LCD with mini-LED backlight under 96, 24, and 6 local dimming zones, respectively.

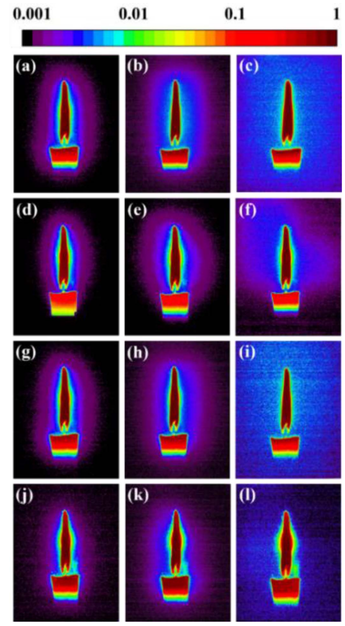

Fig. 8. Normalized luminance distribution of the displayed image "candle" with different numbers of local dimming zones and BL value extraction algorithms. (a), (b), (c), (d), (e), (f), (g), (h), (i), and (j), (k), (l) are the luminance distribution under the maximum method, IMF method, error correction method and average method, respectively. (a), (d), (g), (j), (b), (e), (h), (k), and (c), (f), (i), (l) are the luminance distributions under 96, 24, and 6 local dimming zones, respectively.

possesses the lowest CR under the same number of local dimming zones. The increase in the number of local dimming zones leads to a reduction in the area of each zone, enhancing the halo effect and decreasing CR. Therefore, CR decreases with increasing the number of local dimming zones (patterns I-III in Tables I and II), which is identical for both the edge-lit and local dimming LCDs.

B. Halo Effect

In addition to evaluating the CR of the four testing patterns mentioned above, two images shown in Fig. 6 are also selected to compare the luminance distributions between the original edge-lit LCD and the LCD with local dimming mini-LED backlight (Fig. 7). It is found that the LCD with local dimming mini-LED backlight can display high-quality dark in the surrounding area. As the number of local dimming zones increases, the area of halo reduces, demonstrating that the halo effect can be suppressed by increasing the number of local dimming areas, thereby enhancing the HDR of the LCD.

The interplays between BL value extraction algorithm and the halo effect have also been investigated under the 96, 24, and 6 local dimming zones. By employing the abovementioned algorithms, the BL value extraction and pixel compensation have been realized and the halo effect have been investigated by collecting the normalized luminance distribution of LCD. As shown in Fig. 8, under the same BL value extraction method, the halo area gradually shrinks as the number of local dimming zones increases. For the 6 local dimming zones, the MAX method and CORR method possess relatively serious halo effect.

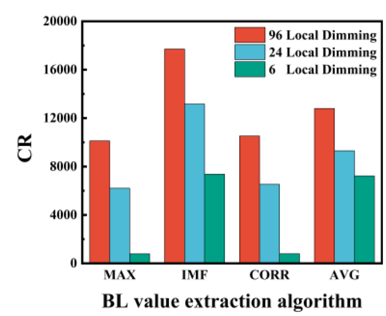

Fig. 9. CR of four BL value extraction algorithms.

The measured values of CR under four BL value extraction methods are shown in Fig. 9. The increase on the number of local dimming zones can improve CR under all of the four methods. Among the four methods, the IMF method possess the highest CR and the MAX method possess the lowest CR. The maximum difference on CR originating from the number of local dimming zones reaches approximately 10000, however, that originating from BL value extraction method reaches approximately 8000, indicating that the impact of the number of local dimming zones is more prominent.

IV. Conclusion

LCD employing local dimming mini-LED backlight has been investigated under different numbers of local dimming zone, as well as different algorithms of BL value extraction. Among the four BL value extraction algorithms investigated in this work, the IMF method possess the highest CR and the MAX method possess the lowest CR. For the same BL value extraction algorithm, the halo area gradually shrinks as the number of local dimming zones increases. Compared with the algorithm of BL value extraction, the number of local dimming zones possesses a more important impact of on CR.

REFERENCES

[1] H. Seetzen et al., "High dynamic range display systems," *ACM Trans. Graph.*, vol. 23, no. 3, pp. 760–768, Aug. 2004, doi: 10.1145/1015706.1015797.

[2] R. Boitard, M. T. Pourazad, P. Nasiopoulos, and J. Slevinsky, "Demystifying high-dynamic-range technology: A new evolution in digital media," *IEEE Consum. Electron. Mag.*, vol. 4, no. 4, pp. 72–86, Oct. 2015, doi: 10.1109/MCE.2015.2463294.

[3] E. L. Hsiang, Q. Yang, Z. Q. He, J. Y. Zou, and S. T. Wu, "Halo effect in high-dynamic-range mini-LED backlit LCDs," *Opt. Exp.*, vol. 28, no. 24, pp. 36822–36837, Nov. 2020, doi: 10.1364/OE.413133.

[4] G. J. Tan, Y. G. Huang, M. C. Li, S. L. Lee, and S. T. Wu, "High dynamic range liquid crystal displays with a mini-LED backlight," *Opt. Exp.*, vol. 26, no. 13, pp. 16572–16584, Jun. 2018, doi: 10.1364/OE.26.016572.

[5] H. W. Chen, J. H. Lee, B. Y. Lin, S. Chen, and S. T. Wu, "Liquid crystal display and organic light-emitting diode display: Present status and future perspectives," *Light Sci. Appl.*, vol. 7, no. 3, Dec. 2017, Art. no. 17168, doi: 10.1038/lsa.2017.168.

[6] Y. G. Huang, E. L. Hsiang, M. Y. Deng, and S. T. Wu, "Mini-LED, Micro-LED and OLED displays: Present status and future perspectives," *Light Sci. Appl.*, vol. 9, no. 1, Jun. 2020, Art. no. 105, doi: 10.1038/s41377-020-0341-9.

[7] G. Hong et al., "A brief history of OLEDs—Emitter development and industry milestones," *Adv. Mater.*, vol. 33, no. 9, Mar. 2021, Art. no. 2005630, doi: 10.1002/adma.202005630.

[8] Z. Yang, E. L. Hsiang, Y. Qian, and S. T. Wu, "Performance comparison between mini-LED backlit LCD and OLED display for 15.6-inch notebook computers," *Appl. Sci.*, vol. 12, no. 3, Jan. 2022, Art. no. 1239, doi: 10.3390/app12031239.

[9] P. Lavole, S. K. Lee, S. J. Kang, and Y. H. Kim, "Dynamic clipping ratio determination for global backlight dimming in LCD," in *Proc. IEEE Int. Symp. Circuits Syst.*, 2010, pp. 3256–3259. doi: 10.1109/ISCAS.2010.5537926.

[10] C. C. Lai and C. C. Tsai, "Backlight power reduction and image contrast enhancement using adaptive dimming for global backlight applications," *IEEE Trans. Consum. Electron.*, vol. 54, no. 2, pp. 669–674, May 2008, doi: 10.1109/TCE.2008.4560145.

[11] Q. B. Feng, H. J. He, D. Han, L. Zhang, and G. Q. Lv, "Image-classification-based global dimming algorithm for LED backlights in LCDs," *Opt. Laser Technol.*, vol. 70, pp. 106–111, Jul. 2015, doi: 10.1016/j.optlastec.2014.12.021.

[12] X. B. Zhang, R. Wang, D. Dong, J. H. Han, and H. X. Wu, "Dynamic backlight adaptation based on the details of image for liquid crystal displays," *J. Display Technol.*, vol. 8, no. 2, pp. 108–111, Feb. 2012, doi: 10.1109/JDT.2011.2165935.

[13] H. Cho and O. K. Kwon, "A backlight dimming algorithm for low power and high image quality LCD applications," *IEEE Trans. Consum. Electron.*, vol. 55, no. 2, pp. 839–844, May 2009, doi: 10.1109/TCE.2009.5174463.

[14] F. C. Lin et al., "Dynamic backlight gamma on high dynamic range LCD TVs," *J. Display Technol.*, vol. 4, no. 2, pp. 139–146, Jun. 2008, doi: 10.1109/JDT.2008.920175.

[15] J. J. Hong, S. E. Kim, and W. J. Song, "A clipping reduction algorithm using backlight luminance compensation for local dimming liquid crystal displays," *IEEE Trans. Consum. Electron.*, vol. 56, no. 1, pp. 240–246, Feb. 2010, doi: 10.1109/TCE.2010.5439151.

[16] G. W. Yoon, S. W. Bae, Y. B. Lee, and J. B. Yoon, "Edge-lit LCD backlight unit for 2D local dimming," *Opt. Exp.*, vol. 26, no. 16, pp. 20802–20812, Aug. 2018, doi: 10.1364/OE.26.020802.

[17] T. Zhang, Y. F. Wang, H. Y. Wu, M. Li, and Z. C. Lei, "High-performance local-dimming algorithm based on image characteristic and logarithmic function," *J. Soc. Inf. Display*, vol. 27, no. 2, pp. 85–100, Feb. 2019, doi: 10.1002/jsid.740.

[18] W. S. Oh, D. Cho, K. M. Cho, G. W. Moon, B. Yang, and T. Jang, "A novel two-dimensional adaptive dimming technique of X-Y channel drivers for LED backlight system in LCD TVs," *J. Display Technol.*, vol. 5, no. 1, pp. 20–26, Jan. 2009, doi: 10.1109/JDT.2008.2004358.

[19] S. Cha, T. Choi, H. Lee, and S. Sull, "An optimized backlight local dimming algorithm for edge-lit LED backlight LCDs," *J. Display Technol.*, vol. 11, no. 4, pp. 378–385, Apr. 2015, doi: 10.1109/JDT.2015.2401604.

[20] T. Z. Wu et al., "Mini-LED and Micro-LED: Promising candidates for the next generation display technology," *Appl. Sci.*, vol. 8, no. 9, Sep. 2018, Art. no. 1557, doi: 10.3390/app8091557.

[21] Y. L. Li and Y. T. Liu, "MicroLED display: The next-generation display technology," *Proc. SPIE*, vol. 11304, pp. 72–75, Feb. 2020. doi: 10.1117/12.2548417.

[22] K. Behrman and I. Kymissis, "Micro light-emitting diodes," *Nature Electron.*, vol. 5, no. 9, pp. 564–573, Sep. 2022, doi: 10.1038/s41928-022-00828-5.

[23] R. D. Zhu, Z. Y. Luo, H. W. Chen, Y. J. Dong, and S. T. Wu, "Realizing Rec 2020 color gamut with quantum dot displays," *Opt. Exp.*, vol. 23, no. 18, pp. 23680–23693, Sep. 2015, doi: 10.1364/OE.23.023680.

[24] X. C. Wang, Z. Bao, Y. C. Chang, and R. S. Liu, "Perovskite quantum dots for application in high color gamut backlighting display of light-emitting diodes," *ACS Energy Lett.*, vol. 5, no. 11, pp. 3374–3396, Nov. 2020, doi: 10.1021/acsenergylett.0c01860.

[25] Z. Y. Luo, D. M. Xu, and S. T. Wu, "Emerging quantum-dots-enhanced LCDs," *J. Display Technol.*, vol. 10, no. 7, pp. 526–539, Jul. 2014, doi: 10.1109/JDT.2014.2325218.

[26] W. Y. Zhang et al., "Uniformity improvement of a mini-LED backlight by a quantum-dot color conversion film with nonuniform thickness," *Opt. Lett.*, vol. 48, no. 21, pp. 5643–5646, Nov. 2023, doi: 10.1364/OL.505552.

[27] H. Chen, J. He, and S. T. Wu, "Recent advances on quantum-dot-enhanced liquid-crystal displays," *IEEE J. Sel. Topics Quantum Electron.*, vol. 23, no. 5, Sep. 2017, Art. no. 1900611, doi: 10.1109/JSTQE.2017.2649466.

[28] L. Kerofsky and S. Daly, "Brightness preservation for LCD backlight dimming," *J. Soc. Inf. Display*, vol. 14, no. 12, pp. 1111–1118, 2006, doi: 10.1889/1.2408394.

[29] S. J. Song, Y. I. Kim, J. Bae, and H. Nam, "Deep-learning-based pixel compensation algorithm for local dimming liquid crystal displays of quantum-dot backlights," *Opt. Exp.*, vol. 27, no. 11, pp. 15907–15917, May 2019, doi: 10.1364/OE.27.015907.

[30] L. Duan, D. Marnerides, A. Chalmers, Z. Lei, and K. Debattista, "Deep controllable backlight dimming for HDR displays," *IEEE Trans. Consum. Electron.*, vol. 68, no. 3, pp. 191–199, Aug. 2022, doi: 10.1109/TCE.2022.3188806.

[31] Z. W. Gao et al., "Mini-LED backlight technology progress for liquid crystal display," *Crystals*, vol. 12, no. 3, Feb. 2022, Art. no. 313, doi: 10.3390/cryst12030313.

[32] E. G. Chen et al., "Metamaterials for light extraction and shaping of micro-scale light-emitting diodes: From the perspective of one-dimensional and two-dimensional photonic crystals," *Opt. Exp.*, vol. 31, no. 11, pp. 18210–18226, May 2023, doi: 10.1364/OE.489598.

[33] Z. B. Lin et al., "Zero-optical-distance mini-LED backlight with cone-shaped light coupling microstructures," *Crystals*, vol. 13, no. 2, Jan. 2023, Art. no. 241, doi: 10.3390/cryst13020241.

[34] E. G. Chen et al., "Edge/direct-lit hybrid mini-LED backlight with U-grooved light guiding plates for local dimming," *Opt. Exp.*, vol. 29, no. 8, pp. 12179–12194, Apr. 2021, doi: 10.1364/OE.421346.

[35] E. L. Hsiang, Z. Y. Yang, Q. Yang, Y. F. Lan, and S. T. Wu, "Prospects and challenges of mini-LED, OLED, and micro-LED displays," *J. Soc. Inf. Display*, vol. 29, no. 6, pp. 446–465, 2021, doi: 10.1002/jsid.1058.

[36] B. Kim, J. Kim, W. S. Ohm, and S. Kang, "Eliminating hotspots in a multi-chip LED array direct backlight system with optimal patterned reflectors for uniform illuminance and minimal system thickness," *Opt. Exp.*, vol. 18, no. 8, pp. 8595–8604, Apr. 2010, doi: 10.1364/OE.18.008595.

[37] L. Y. Liao and Y. P. Huang, "Blur-mask approach for real-time calculation of light spreading function (LSF) on spatial modulated high dynamic range LCDs," *J. Display Technol.*, vol. 6, no. 4, pp. 121–127, Apr. 2010, doi: 10.1109/JDT.2009.2035826.

[38] S. E. Kim, J. Y. An, J. J. Hong, T. W. Lee, C. G. Kim, and W. J. Song, "How to reduce light leakage and clipping in local-dimming liquid-crystal displays," *J. Soc. Inf. Display*, vol. 17, no. 12, pp. 1051–1057, Dec. 2009, doi: 10.1889/JSID17.12.1051.

[39] A. Konno, Y. Yamamoto, and T. Inuzuka, "40.2: RGB color control system for LED backlights in IPS-LCD TVs," *SID Symp. Dig.*, vol. 36, no. 1, pp. 1380–1383, 2005, doi: 10.1889/1.2036264.

[40] C. C. Chen et al., "17-4: Evaluate and upgrade picture quality of local dimming mini-LED LCD," *Symp Dig. Tech Papers*, vol. 51, no. 1, pp. 235–238, Aug. 2020, doi: 10.1002/sdtp.13847.

[41] Y. G. Huang, G. J. Tan, F. W. Gou, M. C. Li, S. L. Lee, and S. T. Wu, "Prospects and challenges of mini-LED and micro-LED displays," *J. Soc. Inf. Display*, vol. 27, no. 7, pp. 387–401, 2019, doi: 10.1002/jsid.760.